Evaluation of High-Resolution Pinhole SPECT Using a Small Rotating Animal

Jan B.A. Habraken, Kora de Bruin, Morgan Shehata, Jan Booij, Roel Bennink, Berthe L.F. van Eck Smit, and Ellinor Busemann Sokole

Departments of Nuclear Medicine, Radiology, and Medical Technological Development, Academic Medical Center, University of Amsterdam, Amsterdam, The Netherlands

Ex vivo measurements in animals are used frequently in the field of nuclear medicine for the characterization of newly developed radioligands and for drug development. In vivo SPECT would replace these ex vivo measurements in a relatively large number of cases if one were able to adequately image small organs. The pinhole collimator has been used extensively to obtain greater detail in planar imaging. However, using a pinhole collimator for SPECT is difficult because it requires a heavy collimated detector to rotate around a small object with a constant radius of rotation. **Methods:** We have developed a mechanism in which the gantry and collimator are fixed and the animal rotates. Hollow cylinders of different sizes were made to enable imaging of small animals of different sizes: mice, hamsters, and rats. The cylinder is mounted on a stepping motor-driven system and positioned exactly above the pinhole collimator of an ARC3000 camera with a 1-mm pinhole insert. The stepping motor is controlled by the Hermes acquisition/processing system. After imaging each projection, a signal is given to rotate the stepping motor with the desired number of angular degrees. Filtered backprojection, adapted to pinhole SPECT, was used for reconstruction. The system allows adjustments of the radius of rotation and along the axis of the cylinder to select the field of view. Calibration experiments were performed to ensure that the axis of rotation was exactly in the middle of the cylinder. Phantom experiments were performed to assess sensitivity, spatial resolution, and uniformity of the system and to test the system for distortion artifacts. In addition, a brain dopamine transporter rat study and a hamster myocardial study were performed to test the clinical feasibility of the entire system. **Results:** In the line source experiment, the spatial resolution obtained in air was 1.3 mm full width at half maximum, with a radius of rotation of 33 mm. Furthermore, the system has good uniformity and is capable of detecting cold spots of 2-mm diameter. The animal studies showed that it was feasible to image receptors or transporters and organs with sufficient detail in a practical setup. **Conclusion:** A rotating cylinder mechanism for pinhole SPECT is feasible and shows the same characteristics as conventional pinhole SPECT with a rotating camera head, without distortion artifacts. This mechanism permits pinhole SPECT to replace many ex vivo animal experiments.

Key Words: small animal; pinhole; SPECT.

J Nucl Med 2001; 42:1863–1869

During the development of new radiopharmaceuticals, the biologic behavior and dosimetry are studied frequently by ex vivo measurements in animals (*1,2*). However, the benefits of an in vivo technique, such as SPECT, are numerous. SPECT imaging offers the opportunity to obtain measurements at more than 1 point in time after administration of a radiopharmaceutical, which is a significant benefit for the determination of temporal behavior. Likewise, SPECT imaging can be repeated over a long time period on the same animal using serial injections of the radiopharmaceutical, which simplifies the assessment of drug therapy effects. The number of animals needed with an in vivo approach is far less than the number required for ex vivo measurements, in which the animal has to be killed for a single measurement. The smaller number of animals required with an in vivo approach is beneficial from an ethical point of view and may also save research time and, therefore, may be more cost-effective. The cost-effectiveness is an important aspect, especially when genetically manipulated animals are used.

A prerequisite for the replacement of ex vivo experiments by SPECT imaging is that it enables an accurate quantification of tracer uptake and kinetics. Quantification measurements with SPECT in larger animals, such as monkeys, have already been satisfactorily performed by several groups (*3*). However, for in vivo experiments with smaller animals, such as mice, hamsters, or rats, a SPECT system encounters its physical limits for resolution and sensitivity. The pinhole collimator has been used extensively to obtain greater detail in planar imaging. However, the application of pinhole SPECT is difficult because it requires a heavy collimated detector to rotate around a small object with a precisely constant radius of rotation. Small misalignments in this setup of pinhole SPECT will generate a displaced center of rotation and produce artifacts. Li et al. (*4*) showed that a small mechanical shift of 1.2 mm creates severe ring and doughnut-type artifacts. To circumvent this problem, we have developed an animal pinhole SPECT system in which the mechanical misalignment is minimized. The basic concept of the system is that the heavy collimated
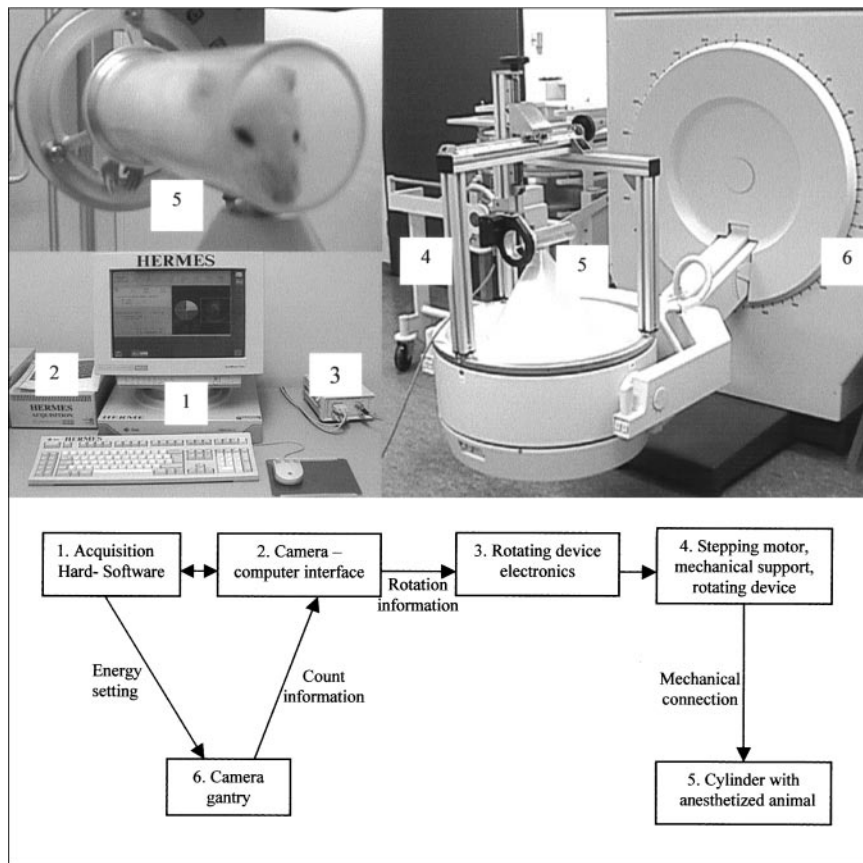
FIGURE 1. Overview and schematic diagram of pinhole SPECT system.

detector is fixed and the lightweight object, the animal or phantom, rotates.

A device was constructed that enables precise positioning of the object in the midline of the pinhole and flexible positioning in the other 2 directions. To ensure that the rotation of the object does not introduce artifacts, calibration experiments were performed. Phantom experiments were done to investigate the extent to which accurate quantification of tracer uptake may be possible with this new system. In vivo experiments were performed using 2 animals of different size, a rat and a hamster, to test the clinical feasibility of the system.

MATERIALS AND METHODS

Mechanical Support of Pinhole SPECT Apparatus

Figure 1 shows the components of the pinhole SPECT apparatus, including the mechanical support, which was constructed at the Department of Medical Technological Development of the Academic Medical Center. The support consists of 3 aluminum vertical legs, which are connected by 2 horizontal rods of the same material. Each vertical leg has a pin with a rubber ring that fits precisely in a corresponding hole on the collimator rim. This connection enables the mechanical support to be mounted easily, with the rods exactly parallel to the collimator and the detector crystal. A fourth adjustable vertical leg is connected on 1 of the horizontal rods. On this leg a ring is mounted, which is driven by

a stepping motor. Three cylinders of different sizes (25-, 38-, and 47-mm diameter)—suitable for mice (20–30 g), hamsters (100–150 g), and rats (150–250 g) as well as several phantoms—can be connected easily to the ring. The animals used for our research experiments have a specified weight with an accuracy of 10%; therefore, a single cylinder can be used for all measurements within 1 experiment. The mechanical support allows easy and precise manual adjustment of the object in 2 directions: the distance of the cylinder to the pinhole aperture, which equals the radius of rotation (ROR), and an adjustment along the axis of the cylinder to select the field of view.

Pinhole SPECT Acquisition Procedure

The object, the cylinder with the animal or phantom, is positioned directly above the pinhole, with a minimum distance. After acquiring data from each projection, according to the step-and-shoot mechanism, a signal from the acquisition station to the stepping motor induces rotation of the object. The stepping motor makes 500 steps per 360° rotation. Because a complete number of steps per projection is necessary, this allows 25, 50, 100, 125, 250, or 500 projections per 360° rotation. The mechanical support was designed so that the midline of the cylinder is exactly in the middle of the pinhole. Thus, the SPECT acquisition can be regarded as a conventional circular orbit acquisition with a rotating camera head. However, in this case, the cylinder midline equals the axis of rotation, and the distance from the cylinder midline to the pinhole aperture equals the ROR. Because the cylinder rotates exactly

around its midline, the ROR is not affected by a rotation-induced variation, which is essential for pinhole SPECT acquisition.

Acquisition Parameters

An ARC3000 scintillation camera (ADAC Laboratories, Milpitas, CA) was used with a circular field-of-view diameter of 400 mm. The pinhole collimator had a diameter of 300 mm and an opening angle of 60° (distance between the aperture and the detector is 260 mm). For the sensitivity measurements, a pinhole insert of 1-mm aperture size was compared with a 2-mm insert. In all other experiments, a tungsten pinhole insert with a 1-mm aperture was used. All experiments were acquired with a 20% energy window, 127–155 keV for ^{99m}Tc experiments and 143–175 keV for ^{123}I experiments. A Hermes workstation (Nuclear Diagnostics, Stockholm Sweden) was used to control the camera and the stepping motor.

Reconstruction

The reconstruction was performed using a HERMES application program (Nuclear Diagnostics); this application uses filtered backprojection, adapted to pinhole SPECT, according to the conversion algorithm of Feldkamp et al. (5). The ramp filter was used as a reconstruction filter in all experiments. Unless a specific smoothing filter is mentioned in the study description, no postreconstruction filter was used.

Calibration and Phantom Studies

Calibration Phantom. The calibration phantom is a cylinder with a line source positioned exactly along the central axis of the cylinder. The line source, 6 cm long with a 0.2-mm internal diameter, was filled with 1,502 MBq/mL [99m]Tc. Planar acquisitions (128 × 128 matrix size) of the calibration phantom were made to adjust the analog digital converter of the camera–computer interface, such that the line source, at the axis of rotation, was exactly in the middle of the image matrix. This calibration is required to ensure that the transformation to conventional pinhole SPECT data is correct. The calibration needs to be done only after a service of camera or computer interface. Furthermore, to quantify our visual observation that the cylinder did not wobble during rotation, we acquired 100 projections (128 × 128; 15 s per projection; ROR, 25 mm) of the line source. All projection images were added and the spatial resolution, full width at half maximum (FWHM), was measured at the beginning, middle, and end of the line source and compared with the equivalent FWHM measurements from a single projection. We note that the line source was not entirely in the field of view; therefore, the beginning of the line source was defined as the edge of the field of view nearest to where the cylinder was mounted to the stepping motor.

Multiple Line Source Phantom. The multiple line source phantom contains 54 line sources, in free air, at 4-mm distances from each other. Line sources, 6 cm long with a 0.2-mm inner diameter, were filled with 1,502 MBq/mL [99m]Tc. A SPECT acquisition was made (100 projections; 128 × 128; 45 s per projection; ROR, 33 mm) to test the resolution at different locations and to check for distortion artifacts. FWHM values were calculated using 1-pixel-wide line profiles.

Flood Source Phantom. The flood source phantom is a cylinder, 6.8 cm long with a 2.4-cm inner diameter. The cylinder was filled with 3.3 MBq/mL [99m]Tc. The SPECT acquisition (50 projections; 64 × 64; 15 s per projection; ROR, 33 mm) was reconstructed using a Butterworth postreconstruction filter (7.8 cycles per centimeter; order, 5). Using this ROR of 33 mm, only 3.8 cm of the 6.8-cm-long cylinder was in the field of view. SPECT uniformity after reconstruction was only assessed visually and was not quantified because it depends on count statistics, matrix size, and postreconstruction filter (6).

Cold Spot Phantom. The cold spot phantom is a cylinder, 6.8 cm long with a 3.7-cm inner diameter, containing 6 different acrylic inserts of 2-, 3-, 4-, 5-, 6-, and 7-mm diameter. The cylinder was filled with 21.5 MBq/mL [99m]Tc. SPECT acquisition (125 projections; 128 × 128; 20 s per projection; ROR, 38 mm) was reconstructed with a Butterworth postreconstruction filter (9.9 cycles per centimeter; order, 5).

Sensitivity Measurements. Sensitivity of the pinhole SPECT system was measured with the 1- and 2-mm pinhole inserts. A point source of 7.9 MBq ^{99m}Tc was imaged at several distances from the pinhole aperture.

Animal Studies

Feasibility studies were performed with 2 different animals and radionuclides. The animals participated in ongoing trials using planar scintigraphy and ex vivo counting. A rat was imaged 2 h after injection of 74 MBq ^{123}I-labeled *N*-ω-fluoropropyl-2β-carbomethoxy-3β-(4-iodophenyl)nortropane (FP-CIT). [^{123}I]FP-CIT binds to dopamine transporters, which are specifically localized in the membrane of the dopaminergic terminals in the striata. Region-of-interest analysis was used to obtain the uptake ratio between striata and cerebellum (a brain region devoid of dopamine transporters). In addition, a hamster was imaged 1 h after injection of 40 MBq ^{123}I-labeled metaiodobenzylguanidine (MIBG). [^{123}I]MIBG is bound by the amine uptake mechanism in the cell membrane of cathecholaminergic cells in the myocardium. The rat and the hamster were anesthetized before they were pulled tightly into the matching cylinder, such that rotation did not induce movement. A SPECT acquisition (50 projections; 64 × 64; 30 s per projection) was made of each animal. For the rat study, an ROR of 45 mm was used; for the hamster study, an ROR of 33 mm was used. For both studies, a Butterworth postreconstruction filter (4.7 cycles per centimeter; order, 5) was applied.

RESULTS

Phantom Studies

Calibration Phantom. The measured FWHM spatial resolution of a single projection at the beginning, middle, and end of the line source was 1.10, 1.10, and 1.11 mm, respectively. The measured FWHM spatial resolution of all summed projections at the beginning, middle, and end of the line source was 1.09, 1.11, and 1.10 mm, respectively.

Multiple Line Source Phantom. A transverse slice of the multiple line source phantom, at the center of the pinhole, is shown in Figure 2.. It can be seen that distortion artifacts did not influence the result. To quantify this observation, we measured the FWHM spatial resolution in tangential and radial directions for the 16 line sources in 1 quadrant. The average FWHM ± SD for the tangential direction was 1.31 ± 0.14 and that for the radial direction was 1.32 ± 0.08 mm. To test whether the resolution was uniform over the axial direction, the FWHM spatial resolution was measured at 20 positions of a line source in the center of the cylinder. Figure 3 shows the result of these FWHM measurements, where the average FWHM was 1.38 ± 0.14 mm.
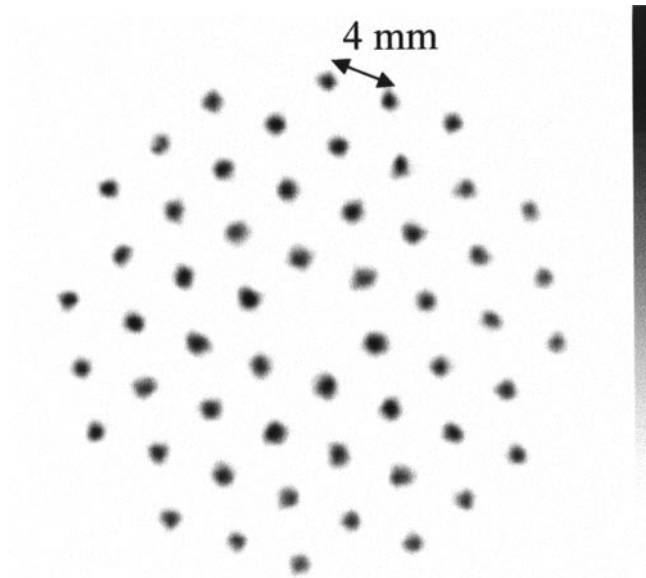
FIGURE 2. Transverse slice of multiple line source phantom.

TABLE 1
Results of Resolution Measurements

FWHM (mm)		Axial distance from pinhole center (mm)	FWHM (mm)
Tangential	Radial		
1.22	1.22	−13.4	1.54
1.25	1.31	−11.9	1.28
1.54	1.34	−10.4	1.29
1.28	1.34	−8.9	1.41
1.28	1.28	−7.4	1.13
1.19	1.19	−5.9	1.60
1.22	1.28	−4.5	1.37
1.28	1.30	−3.0	1.32
1.13	1.46	−1.5	1.33
1.19	1.22	0	1.34
1.34	1.30	1.5	1.56
1.57	1.43	3.0	1.45
1.31	1.46	4.5	1.29
1.25	1.28	5.9	1.53
1.37	1.34	7.4	1.39
1.60	1.34	8.9	1.60
		10.4	1.41
		11.9	1.13
		13.4	1.24
		14.9	1.42

The results of the resolution measurements are presented in Table 1. The average FWHM spatial resolution of all described measurements was 1.34 ± 0.13 mm.

Flood Source Phantom. No nonuniformity artifacts were seen on the transverse and coronal reconstruction slices of the flood source phantom, as shown in Figure 4.

Cold Spot Phantom. From the transverse reconstruction of the cold spot phantom (Fig. 5), all cold spots with a diameter of ≥2 mm were clearly visible.

Sensitivity Measurements. Table 2 shows the results of the sensitivity measurements. The linear relationship between sensitivity and the square of the ratio between the pinhole aperture and distance is shown in Figure 6.

Animal Studies

The rat and the hamster fit tightly in the matching cylinder; no movement of either animal was seen during acquisition. A transverse slice of the [123I]FP-CIT rat brain study is shown in Figure 7. The resolution and contrast of measured uptake in the striata versus the background in surrounding tissue show the feasibility for in vivo quantification of the pinhole SPECT system for this type of study. The measured uptake ratios for left and right striatum compared with cerebellum were 3.47 and 3.32, respectively. Figure 8 shows transverse, coronal, and sagittal slices of the [123I]MIBG hamster study. The left and right myocardial
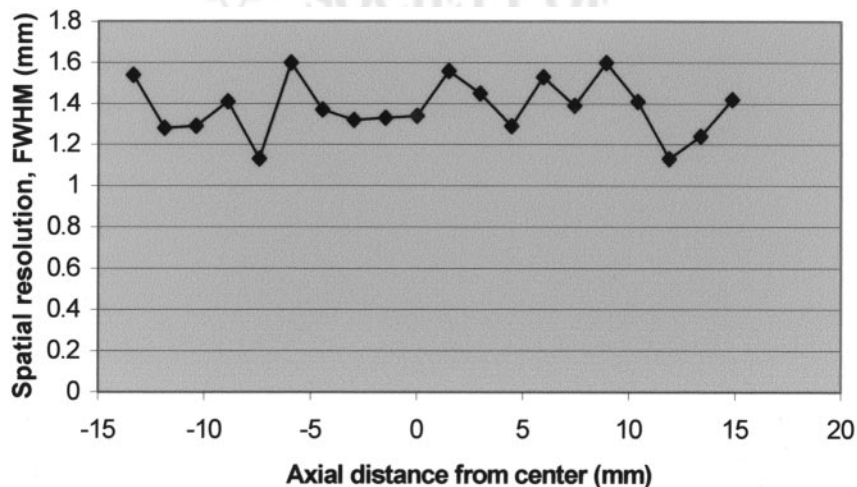

FIGURE 3. Spatial resolution (FWHM) of center line source from beginning to end of cylinder. Axial distance 0 equals center of pinhole.
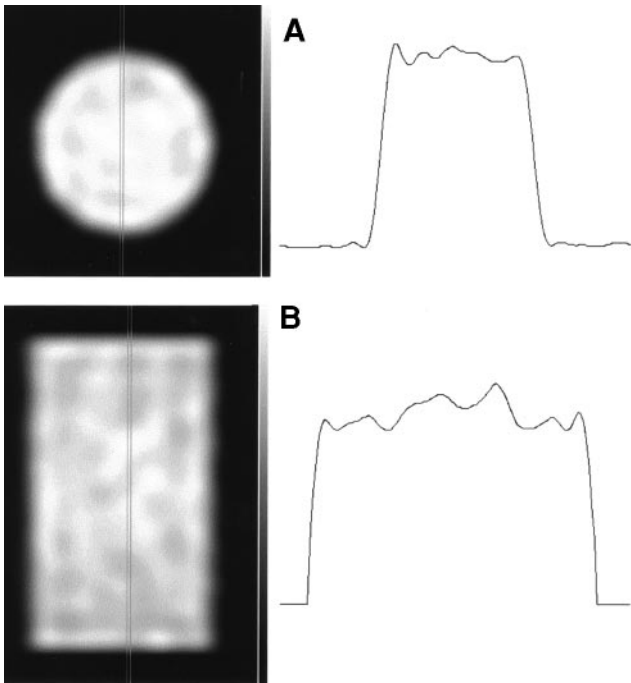
FIGURE 4. (A) Transverse slice of flood source phantom, with profile. (B) Coronal slice of flood source phantom, with profile.

ventricles are clearly visible. Figure 8 does not show artifacts or a significant loss in image quality that could be induced by internal motion of the myocardium.

DISCUSSION

Developments in clinical research, such as gene therapy, have resulted in an increased interest in the in vivo imaging of small animals. Dedicated systems for imaging small
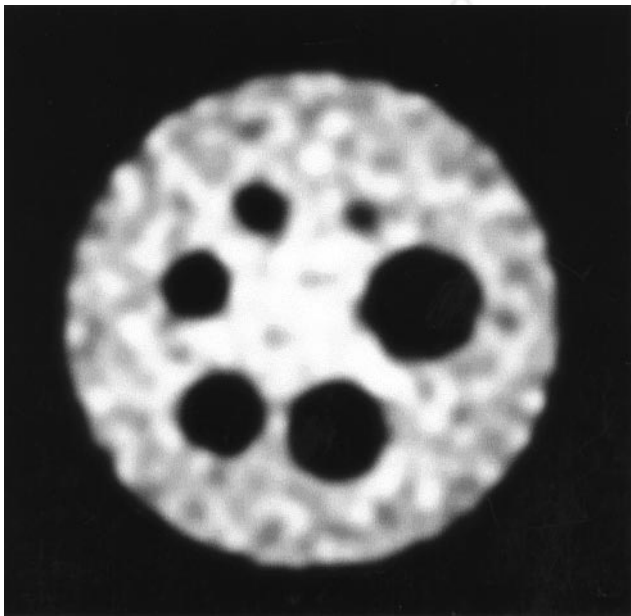

FIGURE 5. Transverse slice of cold spot phantom.

TABLE 2
Results of Sensitivity Measurements

Pinhole aperture (mm)	Distance (mm)	Sensitivity (cps/MBq)
2	16.2	13.1
2	11.2	22.4
2	6.2	63.7
2	3.7	168.8
2	2.7	305.9
2	1.7	735.4
1	16.1	6.8
1	11.1	8.9
1	6.1	20.3
1	3.6	48.5
1	2.6	87.8
1	1.6	216.1

animals have been designed for some imaging modalities such as MRI, CT, and PET (7–11). However, SPECT is an essential modality because it offers the possibility of imaging radioligands with specific receptor binding. An advantage of pinhole SPECT is that a general-purpose camera can be used for ultra-high-resolution experiments for in vivo quantification with small animals. One of the problems of pinhole SPECT for imaging small animals is that slight mechanical shifts or instabilities of only 1 mm cause severe distortion artifacts (4). Reconstruction methods that correct for an angular independent mechanical shift have been presented in the past (4). However, using such a correction method implies that all misalignments are known precisely and behave exactly like the theoretic model. For instance, the proposed method of Li et al. (4) will not correct for an angular dependent mechanical shift. In other words, correction methods can only partially solve this problem. Therefore, we designed a small-animal pinhole SPECT system in which the instabilities are minimized. The basic concept of
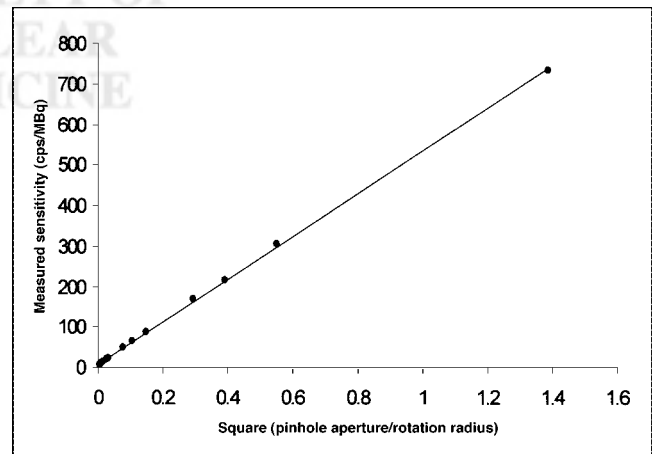

FIGURE 6. Sensitivity of pinhole SPECT equipment plotted against square of ratio between aperture and distance. cps = counts/second.
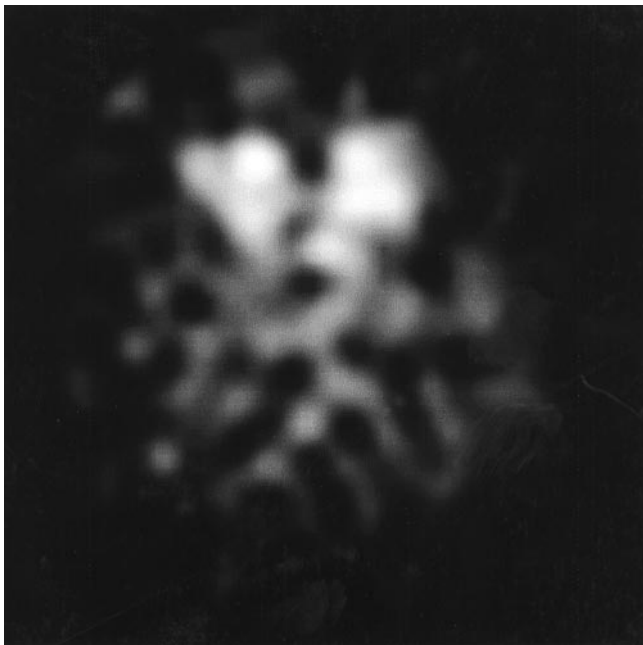
FIGURE 7. Transverse slice of [¹²³I]FP-CIT rat brain study at level of striatum.

the original idea, in which the animal rotates instead of the camera head, was presented earlier (12). Using a line source in the middle of the cylinder, we proved that, during rotation, the midline of the rotating cylinder stays at exactly the same location: The FWHM spatial resolution of the summed projections of the line source was equal to the FWHM of a single projection. This validation was required to ensure that the transformation of the acquisition study to a conventional pinhole SPECT study, with rotating gantry, would not cause distortion artifacts.

According to a calculation based on geometric considerations, the theoretic optimal resolution to be achieved with a 1-mm insert equals approximately 1.2 mm (13). Using a multiple line source phantom, we measured a resolution of 1.34 mm, which is a substantial improvement compared with the resolution of 1.65 mm measured by Ishizu et al. (14) with a conventional dedicated 4-head, pinhole SPECT system. More important, our system did not show any distortion in image linearity. Even in the peripheral area of the reconstructed image the radial spatial resolution equals the tangential spatial resolution. Furthermore, we showed that the spatial resolution was consistent in an axial field of view up to at least 3 cm. The flood source phantom experiment showed that the sensitivity of the system is uniform in the axial and the transaxial directions, which is an essential feature for quantification. The experiment with the cold spot phantom showed that the system is capable of detecting cold spots with a diameter of 2 mm.

The sensitivity of our pinhole SPECT system was proven to behave exactly like the theoretic formula: A linear relationship exists between the sensitivity and the square of the ratio between the pinhole aperture diameter and the distance between the object and pinhole aperture (15). In contrast to some dedicated pinhole SPECT systems, we are entirely free to adjust the ROR. For example, we chose an ROR of 25 mm for mice experiments, whereas Ishizu et al. (14) were limited to a minimum ROR of 40 mm. In other words, the decrease in sensitivity of having a single-head system instead of a multihead system will be balanced partly by the fact that we can use a smaller ROR. Unfortunately, sensitivity will continue to be a limiting factor for using pinhole SPECT for dynamic SPECT studies. Therefore, it might be essential to sacrifice spatial resolution for an increased sensitivity using an insert with a larger aperture.

The feasibility of our pinhole SPECT system was studied with a rat and hamster experiment using ¹²³I-FP-CIT and ¹²³I-MIBG as radioligands. This preliminary study showed that the system is easy to use and that the animals were easily pulled tightly in the cylinder such that rotation did not cause motion of the animal. Furthermore, the result of the myocardial uptake study showed that motion of internal organs, such as the myocardium, induced by rotation did not influence the image quality. Both animal studies were performed with a specialized radiopharmaceutical; consequently, the results do not prove the applicability of our system for abdominal studies with more uniformly distributed pharmaceuticals.

Several improvements to our rotating animal pinhole SPECT concept might be considered. We chose a horizontal positioning of the cylinder because it enabled a stable and consistent mounting of the mechanical support, with the rotating cylinder, onto the collimated camera head. This implied that we had to exclude any motion of the animal or internal organs induced by the rotation. However, other
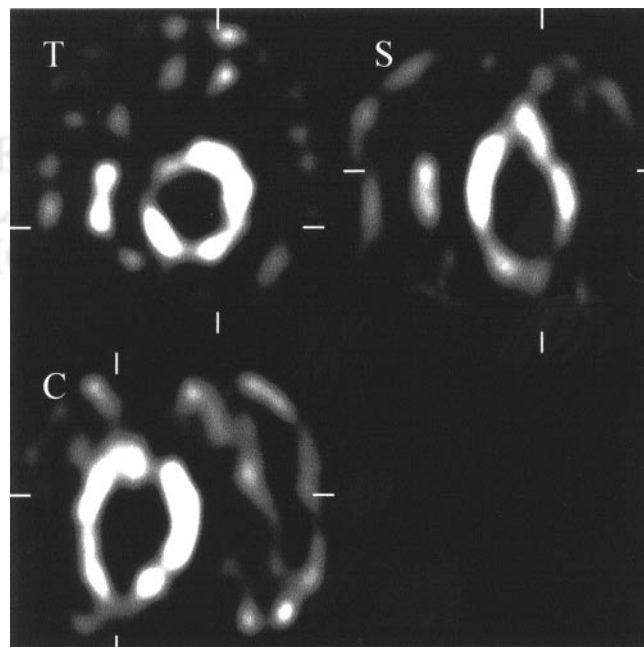

FIGURE 8. Transverse (T), sagittal (S), and coronal (C) views of [¹²³I]MIBG hamster myocardial study.

groups that plan to use the principle of a rotating object for pinhole SPECT might consider a vertical positioning of the cylinder. Furthermore, we arbitrarily adopted a stepping motor with 500 steps per rotation, which limited us to 50, 100, or 125 projections per rotation, whereas a stepping motor of 360 steps per rotation would bring the number of projections per rotation to the more commonly used 60 or 120. In this study, filtered backprojection was used for reconstruction. However, iterative reconstruction has been implemented for pinhole SPECT and has been shown to significantly improve image quality and resolution (*16*). Therefore, we plan to implement iterative reconstruction.

CONCLUSION

The concept of pinhole SPECT using a rotating object and a fixed collimated camera head is technically feasible and enables SPECT imaging of small animals. Using this procedure, we circumvent the problem of mechanical shift and unknown instabilities in a practical, easy-to-use, and low-cost environment. Therefore, pinhole SPECT may be used more extensively for the assessment of in vivo uptake of radioligands in small animals and may replace many in vitro experiments.

REFERENCES

1. Booij J, Andringa G, Rijks LJM, et al. [123I]FP-CIT binds to the dopamine transporter as assessed by biodistribution studies in rats and SPECT studies in MPTP-lesioned monkeys. *Synapse.* 1997;27:183–190.
2. Rijks LJ, Booij J, Doornbos T, et al. In vitro and in vivo characterization of newly developed iodinated 1-[2-[bis(4-fluorophenyl)methoxy]ethyl]piperazine derivatives in rats: limited value as dopamine transporter SPECT ligands. *Synapse.* 1996;23:201–207.
3. Vermeulen RJ, Drukarch B, Verhoeff NP, et al. No direct correlation between behaviorally active doses of the dopamine D2 agonist LY-171555 and displacement of [123I]IBZM as measured with SPECT in MPTP monkeys. *Synapse.* 1994;17:115–124.
4. Li J, Jaszczak RJ, Greer KL, Coleman RE. A filtered backprojection algorithm for pinhole SPECT with a displaced centre of rotation. *Phys Med Biol.* 1994;39:165–176.
5. Feldkamp LA, Davis LC, Kress JW. Practical cone-beam algorithm. *J Opt Soc Am.* 1984;1:612–619.
6. National Electric Manufacturers Association (NEMA). *Performance Measurements of Scintillation Cameras.* Standards publication NU-1–1994. Washington, DC: NEMA; 1994.
7. Ziegler SI, Pichler BJ, Boening G, et al. A prototype high-resolution animal positron tomograph with avalanche photodiode arrays and LSO crystals. *Eur J Nucl Med.* 2001;28:136–143.
8. Paulus MJ, Gleason SS, Kennel SJ, Hunsicker PR, Johnson DK. High resolution x-ray computed tomography: an emerging tool for small animal cancer research. *Neoplasia.* 2000;2:62–70.
9. Guzman R, Lovblad KO, Meyer M, Spenger C, Schroth G, Widmer HR. Imaging the rat brain on a 1.5 T clinical MR-scanner. *J Neurosci Methods.* 2000;97:77–85.
10. Chatziioannou AF, Cherry SR, Shao Y, et al. Performance evaluation of micro-PET: a high-resolution lutetium oxyorthosilicate PET scanner for animal imaging. *J Nucl Med.* 1999;40:1164–1175.
11. Weber S, Terstegge A, Herzog H, et al. The design of an animal PET: flexible geometry for achieving optimal spatial resolution or high sensitivity. *IEEE Trans Med Imaging.* 1997;16:684–689.
12. Habraken JBA, de Bruin K, Maripuu E, et al. High resolution pinhole SPECT using a small rotating animal [abstract]. *Eur J Nucl Med.* 1999;26(suppl):1018.
13. Weber DA, Ivanovic M. Pinhole SPECT: ultra-high resolution imaging for small animal studies. *J Nucl Med.* 1995;36:2287–2289.
14. Ishizu K, Mukai T, Yonekura Y, et al. Ultra-high resolution SPECT system using four pinhole collimators for small animal studies. *J Nucl Med.* 1995;36:2282–2287.
15. Weber DA, Ivanovic M, Franceschi D, et al. Pinhole SPECT: an approach to in vivo high resolution SPECT imaging in small laboratory animals. *J Nucl Med.* 1994;35:342–348.
16. Vanhove C, Defrise M, Franken PR, Everaert H, Deconinck F, Bossuyt A. Interest of the ordered subsets expectation maximization (OS-EM) algorithm in pinhole single-photon emission tomography reconstruction: a phantom. *Eur J Nucl Med.* 2000;27:140–146.